Shear Rheology of Diluted Solutions of High Molecular Weight Cellulose

P. NAVARD and J. M. HAUDIN, *Ecole Nationale Supérieure des Mines de Paris, U.A. CNRS 852, Sophia Antipolis, 06565 Valbonne Cédex, France* and I. QUENIN and A. PEGUY, *Centre de Recherche sur les Macromolécules Végétales, L.P. CNRS 5301, B.P. 68, 38402 Saint Martin D'Heres Cédex, France*

Synopsis

A steady-state and dynamical rheological study was performed with dilute solutions (1–4%) of high molecular weight cellulose (M_w = 350,000). The solutions are strongly viscoelastic. The steady-state viscosity and the first normal stress difference have a power law dependence on the shear rate. The power law indices have the same dependence on temperature and concentration. These results as well as the correlation between the steady-state viscosity and the real part of the complex viscosity are in good agreement with the Spriggs model. The 4% concentrated solution shows the beginning of a rubber-like storage modulus plateau, suggesting the existence of an entanglement network.

INTRODUCTION

Owing mainly to the lack of suitable solvents, few studies have been published on the rheological properties of cellulose solutions.[1,2] Only recently have new solvents been discovered making possible the manufacture of cellulose products. The major solvents are tertiary amine *N*-oxides, like *N*-methylmorpholine *N*-oxide (MMNO) and *N,N*-dimethylethanolamine *N*-oxide (DMEAO). These true solvents have been investigated in our laboratories[3–9] and they lead to the processing of fibers and films.[10,11] Rheological studies have been conducted with low molecular weight cellulose and with cellulose having a degree of polymerization 600 in MMNO.[12,13] At low concentrations, the cellulose solutions behave as semirigid polymer solutions and show the formation of temporary networks. The highest achievable concentrations are mesomorphic, and their rheology presents some noticeable features.[12] All these studies were conducted under steady-state conditions. No dynamical data have been reported for any cellulose solutions. This paper addresses the steady-state and oscillatory investigation of high molecular weight cellulose in MMNO and DMEAO. We undertake this investigation in order to gain more scientific information on the behavior of this natural polymer, and to relate the possible processing of high molecular weight cellulose solutions for obtaining high modulus fibers.[14]

EXPERIMENTAL

Materials

Menoufi cotton cellulose ($\overline{DP}$ 2000) was dewaxed by alcohol-benzene extraction. MMNO from Texaco was purified by recrystallization of the monohy-

Journal of Applied Polymer Science, Vol. 32, 5829–5839 (1986)
 CCC 0021-8995/86/075829-11$04.00

drate from acetone prior to use, as previously described.[3] DMEAO was received as a gift from Dr. R. N. Armstrong, American Enka. The crystallized solvent contained 9% w/w of water. The dissolution of cellulose was performed at 120°C in both solvents. 1% w/w of propylgallate was added as an antioxidant for preventing cellulose degradation. Several concentrations were prepared between 1 and 4% w/w. They were chosen to provide a good spinnability at temperatures lower than 130°C, the temperature above which a strong degradation occurs. The density of the 1% w/w cellulose in MMNO was measured by the floatation method in a CCl_4-cyclohexane mixture and was found to be 1.20 cm^{-3}.

RHEOLOGICAL MEASUREMENTS

Rheological measurements were performed between 75°C (below which the solutions are solid) and 110°C (above which it is difficult to monitor the water content) with an Instron 3250 rheometer, with two geometries, cone-and-plate (cone angle 6°) and eccentric rotating disks (ERD). No detectable degradation occurred during the course of the experiments, based on viscosity measurements taken before and after experiments. This held true even when the solutions were kept at 110°C for about an hour.

In the present study, only shear rheological measurements were made. Steady-state, cone-and-plate, measurements of the torque, and the normal force F_Z give the shear stress σ_{12} and the first normal stress difference $N_1 = \sigma_{11} - \sigma_{q2}$ (σ_{ij} are the components of the stress tensor). The relation between F_Z and N_1 is[15]

$$N_1 = (\sigma_{11} - \sigma_{22}) = 2F_Z/\pi R^2 \tag{1}$$

where R is the cone radius. In the case of a laminar flow, the relation between the torque and σ_{12} is independent of the flow and of the rotation speed. This is not the case for F_Z, which is a function of the rotation speed due to inertial effects. It was shown[16] that the inertial contribution F_i is:

$$F_i = -3\pi\rho\Omega^2R^4/40 \tag{2}$$

with ρ being the density and Ω the rotation speed in rad. sec^{-1}. The inertial contribution is negative and the correction on the measured force F_m has to be positive. So, $F = F_m - F_i = F_m + 3\pi\rho\Omega^2R^4/40$. The first normal stress difference is:

$$N_i = \frac{2F_m}{\pi R^2} + \frac{3\rho\Omega^2R^2}{20} \tag{3}$$

The principle of ERD measurements[15] is to subject the sample to sinusoidal shearing at frequency ω by rotating two eccentric discs. For the geometry considered in this work, the following relations were used.

$$G' = \frac{F_X}{\pi R^2} \times \frac{h}{a} \tag{4}$$

$$G'' = \frac{F_Y}{\pi R^2} \times \frac{h}{a} \tag{5}$$

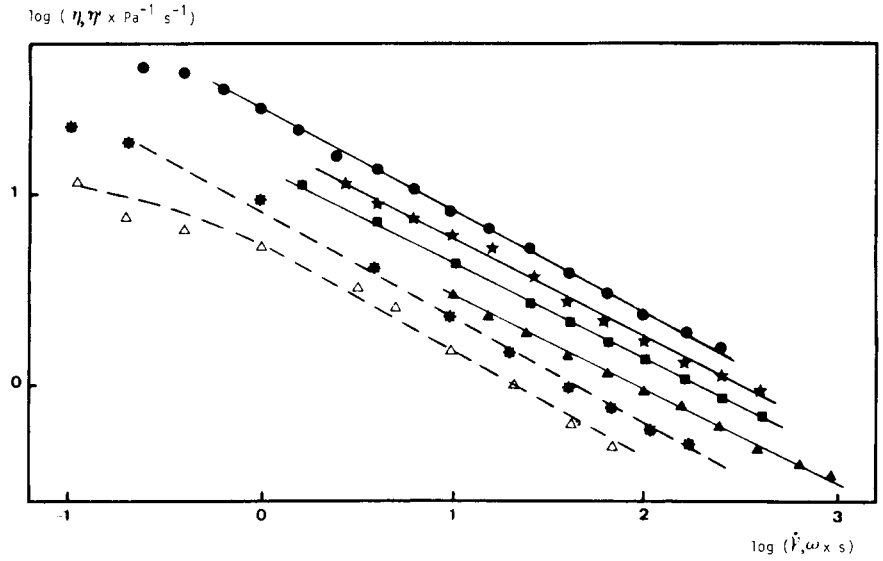

Fig. 1. Steady-state viscosity η and dynamic viscosity η' versus shear rate $\dot{\gamma}$ or frequency ω for a 1% DMEAO solution. η'——* 85%C; △ 105°C; η——● 75°C; ★ 85°C; ■ 95°C; ▲ 105°C.

h is the gap and a is the eccentricity. $a = 0.3$ mm and a/h was set equal to unity. We checked that varying a/h from unity to 0.3 does not change the values of G' and G''.

G' and G'' are the real and imaginary parts of the complex shear modulus. G' is the storage modulus and G'' is the loss modulus. $\eta' = G''/\omega$ and $\eta'' = G'/\omega$ are the real and imaginary parts of the complex viscosity. η' is called the dynamic viscosity. F_X and F_Y are the normal (in the plane containing the two axes) and tangential (perpendicular to this plane) recorded forces.

RESULTS AND DISCUSSIONS

The relation between the shear stress σ_{12} and the shear rate $\dot{\gamma}$, for a laminar flow, as in the case of most polymer solutions, is:

$$\sigma_{12} = K\dot{\gamma}^n \tag{6}$$

K is the consistency and n is the power law index. K and n are constant over some range of shear rate. Such a power law fluid pertains to the class of viscoplastic materials. In this case, the viscosity is defined as $\eta = \sigma_{12}/\dot{\gamma}$:

$$\eta = K\dot{\gamma}^{n-1} \tag{7}$$

An illustration of this behavior is given in Figure 1 for a 1% solution in DMEAO and in Figure 2 for 2.5% solutions in DMEAO and in MMNO. In contrast to many polymer solutions, there is no Newtonian plateau. Such a result for cellulose solutions in MMNO has been previously seen.[11] Note that in this study an extended range of shear rates (10^{-1} s^{-1} < $\dot{\gamma}$ < 10^3 s^{-1}) was employed. It was possible to use very high rotation speeds which are usually

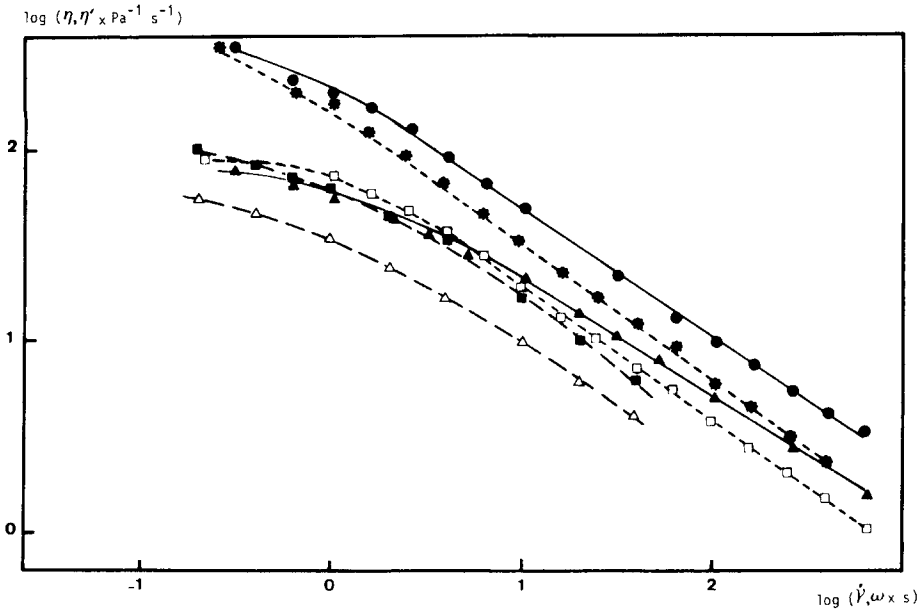

Fig. 2. Steady-state viscosity η and dynamic η' versus shear rate $\dot{\gamma}$ or frequency ω for 2.5% DMEAO and MMNO solutions. DMEAO: η'——■ 85°C; △ 105°C; η——● 75°C; ▲ 105°C. MMNOη----* 75°C; □ 105°C.

not attainable due to the centrifugal force tending to eject the material from the gap. Exceptionally, all the cellulose solutions studied so far have shown this very large stability. The use of these large rotation speeds seems to have no influence on the viscosity measurements, as may be seen from the linearity of the log η versus log $\dot{\gamma}$ curves up to 10^3 s^{-1}. We are unable to ascribe this behavior to a precise physical property. There is no doubt that adhesion forces play a major role. It is anyway a very original and interesting phenomenon.

In Figure 2, at high temperatures, there is a gradual levelling at low shear rates due to the onset of the Newtonian plateau. The fact that this occurs over more than a decade of shear rate may be due to polydispersity, which in our case is unknown. Due to this slow levelling, it was impossible to obtain the plateau viscosity η_o, the shear stress at very low shear rates being much too small to be measured. As found for all concentrations and temperatures, and illustrated in Figure 2, the viscosity of a solution in MMNO is slightly smaller than in DMEAO, holding other parameters constant. This effect is larger at high shear rates. The difference may be explained by a difference in interaction between the cellulose and the two solvents. MMNO has one hydrophilic and one hydrophobic moiety. After solvation of the cellulose molecule by the hydrophilic domain, other interaction between cellulose and the solvent is improbable. On the contrary, DMEAO has two hydrophilic moieties (N → 0 and OH). And thus when the N → 0 part interacts with the cellulose molecule, the DMEAO has another moiety remaining which is capable of forming one hydrogen bond with another DMEAO molecule or with cellulose. This increases the number of intermolecular and interchain bonds in the solution and therefore increases the viscosity.

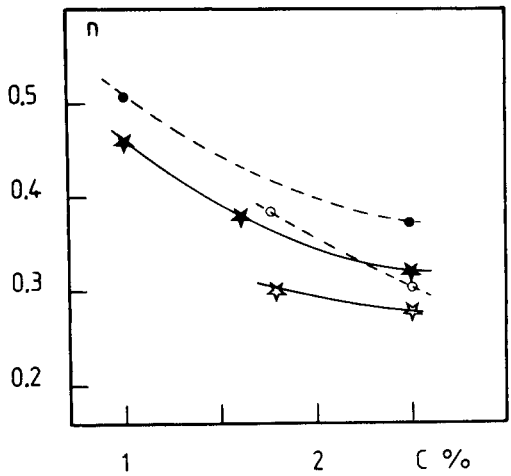

Fig. 3. Power law index n versus concentration C. ★ DMEAO 75°C; ☆ MMNO 75°C; ● DMEAO 105°C; ○ MMNO 105°C.

The power law index n [see Eq. (6)] is plotted in Figure 3. Note that $n = 1$ for a Newtonian behavior and $n = 0$ for a plastic behavior. From Figure 3 one can see that the viscosity of MMNO solutions is more sensitive to shear rate than that of DMEAO solutions. The smallest number of intermolecular bonds in the case of MMNO might favor the formation and deformation of entanglements, usually thought to be the main reason for a power law behavior. The variation of n with concentration and temperature does not allow the plot of a master viscosity curve, as all of the known models invoke a constant n. Moreover, a key parameter for plotting master curves is η_0,[17] which is lacking here. Thus, in our case, the steady-state rheology will not be very useful for the comparison with theoretical predictions.

Figure 4 gives the activation energy of viscous flow E, as a function of $\dot{\gamma}$. E is defined by:

$$\eta = A \exp(E/RT) \tag{8}$$

where A and R are constants. A similar E versus $\dot{\gamma}$ curve was found for concentrated cellulose $\overline{DP}$ 600-MMNO solutions.[12] Equations (7) and (8) give E as a function of $\dot{\gamma}$ and of a small temperature change $\Delta(1/T)$:

$$E/R = (\Delta(\ln K) + \Delta n \ln \dot{\gamma})/\Delta(1/T) \tag{9}$$

Since $\Delta n/\Delta(1/T)$ and $\Delta(\ln K)/\Delta(1/T)$ are independent of $\dot{\gamma}$, E/R should be a linear function of $\log \dot{\gamma}$. This is true when Eq. (7) is obeyed, that is for $\log \dot{\gamma} > 1.5$ for the cellulose solutions. The quasiexponential increase of E when $\log \dot{\gamma}$ decreases implies that the Newtonian plateau (or the end of the levelling) finishes at a higher $\dot{\gamma}$ when the temperature increases.

Oscillatory measurements were carried out with the ERD geometry. Figure 5 gives an example of two measurements with a 4% solution in DMEAO. Due probably to the rather large cone angle used, instabilities occurred for this solution in the cone-and-plate geometry, except at very low shear rates. It was thus possible, for this solution, to have information with the ERD geometry

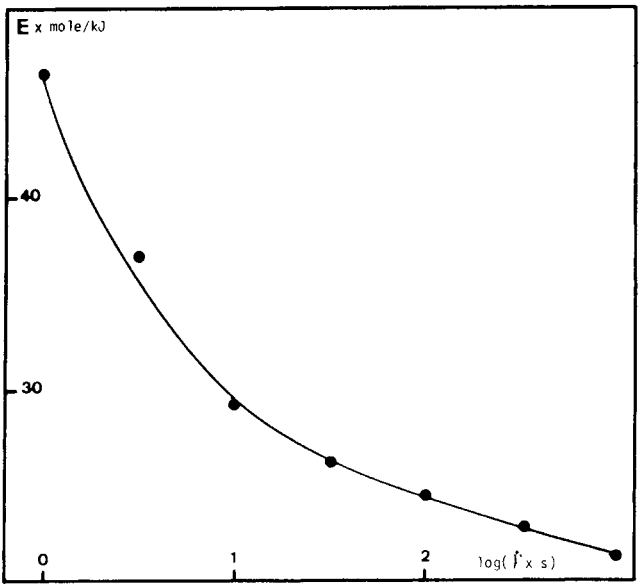

Fig. 4. Activation energy E versus shear rate $\dot{\gamma}$ for a 2.5% DMEAO solution.

where the relative motion of the fluid is much less important. The dynamic viscosity η' shows the same general trend as the steady-state shear viscosity η, i.e., a linear part at high shear rate or frequency, and a levelling at low shear rate or frequency. The storage modulus G' will be analyzed in a later section. The comparison of η with η' is usually very useful. Figures 1 and 2 show the shear dependence of η and η' at a variety of concentrations and temperatures. A usual comparison is to check if $\eta'_{\omega \to o} = \eta_o$. Since we did not

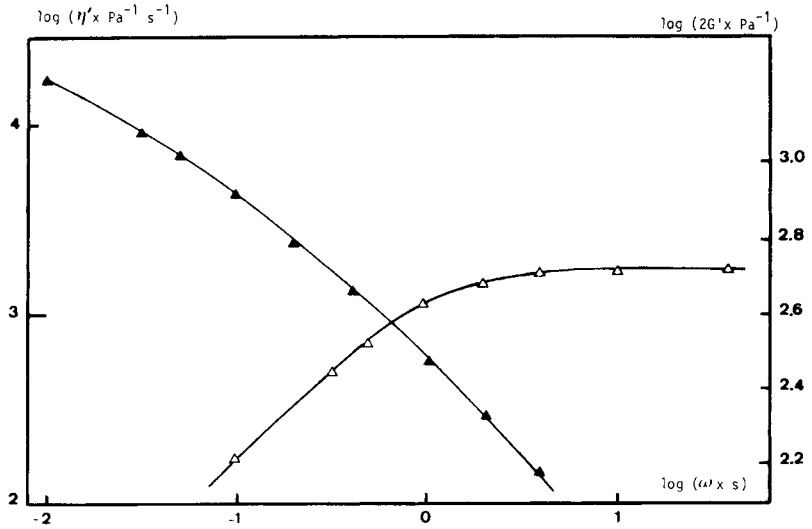

Fig. 5. Dynamic viscosity η' and storage modulus G' versus frequency ω for a 4% DMEAO solution at 105°C. ▲ η'; △ $2G'$.

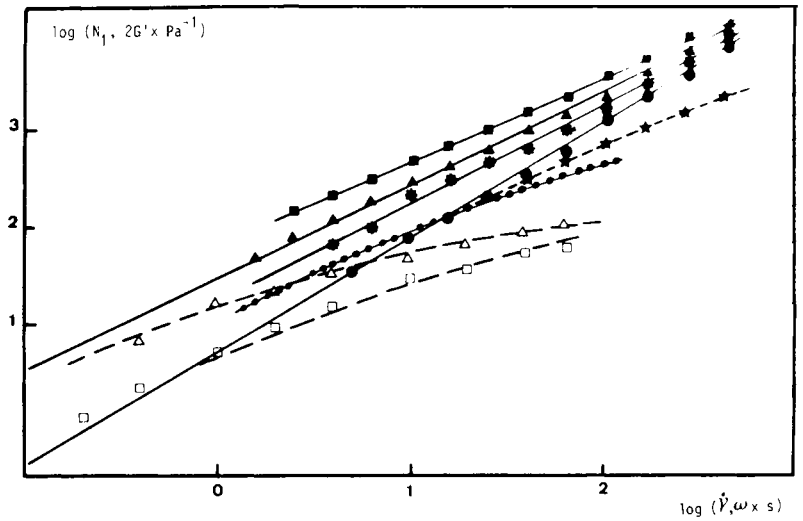

Fig. 6. First normal stress difference N_1 and storage modulus G' versus shear rate $\dot{\gamma}$ or frequency ω for a 1% DMEAO solution. N_1: ■ 75°C; ▲ 85°C; • 94°C; ● 105°C; $2G'$: △ 85°C; □ 105°C. ★ N_1 versus $\dot{\gamma}$ at 105°C without inertial corrections (—●—●—●—●—) $2G'/C^2$ ($C\dot{\gamma}$) at 105°C.

have η_o, it is impossible to make this check. We compare $\eta' = f(\omega)$ and $\eta = f(\dot{\gamma})$ and more precisely see if, by translation along the $\dot{\gamma} - \omega$ axis in a log-log plot, they are superposable. This is actually the case for nearly all the experiments (all results are not shown in the provided figures). The viscosity-shear rate curve is the same as the dynamic viscosity-frequency curve when a shift factor C is used, given by $\eta(C\dot{\gamma}) = \eta'(\omega)$. A shift factor of 0.3 was found. This may be viewed as consistent with the theory of Spriggs.[18,19] The Spriggs' constitutive equation for viscoelastic fluid is based on the generalized Maxwell model, but with a convected derivative given by the author and satisfying material objectivity. In this way, the model predicts a non-Newtonian viscosity and normal stresses under steady simple shear. It also has some other predictions as to the above mentioned one concerning η and η'. The shift factor C is related to one of the four constants of this model. The analogy between η and η' is one of the tests of this model and shows it may fit our results. There are only a few experimental measurements of the value of C. They range from 0.5 to 1.[19,20] The value of $C = 0.3$, being apparently low, is difficult to explain in terms of molecular implications.

As suggested by several theories and often a source of reference, the first normal stress difference N_1 is equal to twice the storage modulus G' when $\dot{\gamma} \to 0$. N_1 and $2G'$ are plotted in Figure 6 for the 1% solution in DMEAO. It was not possible to measure N_1 at low enough shear rates to be able to unambiguously evaluate this relation. However, an extrapolation of the results suggests that the relationships may hold true. In Figure 6, N_1 has a power index in the 0.8–1.2 range. This measurement was corrected for the inertial contribution of Eq. (2). A comparison of the N_1 versus $\dot{\gamma}$ plot with and without correction is given for $T = 105$°C in Figure 6. The first normal stress difference is, at low shear rate, a quadratic function of the shear rate. This is

predicted by all of the molecular and continuum theories. This is not the case for the studied solutions, where N_1 is a power law function of $\dot{\gamma}$, with a power index in the range 0.8–1.2. The Spriggs' model predicts a strong connection between the behavior of η and N_1. At low shear rate, $\eta \simeq \dot{\gamma}$ and $N_1 \simeq \dot{\gamma}^2$ while above a certain critical shear rate, $\eta \simeq \dot{\gamma}^n$ and $N_1 \simeq \dot{\gamma}^n$. This is obviously not the case (see fig. 3) and this is the most serious disagreement we found. But, as will be seen in the discussion on the relaxation time, there is a strong correlation between the power law indices of η and N_1 when the concentration or the temperature are changed. G' shows a viscous shape for the less concentrated solution in Figure 6. For the most concentrated (4%), a rubberlike plateau is clearly seen above 10 s^{-1} in Figure 5, expressing the influence of entanglements in the solution.

As for the comparison of η and η', the Spriggs' theory predicts a relation between the storage modulus G' and the first normal stress difference N_1. According to this theory,

$$\frac{G'(\omega)}{\omega\eta_0} = \frac{\omega\lambda}{Z}A(\omega) \tag{10}$$

$$\frac{N_1(\dot{\gamma})}{2\lambda\eta_0\dot{\gamma}^2} = \frac{1}{Z}A(C\dot{\gamma}) \tag{11}$$

A, λ, Z are constants or functions of ω or $\dot{\gamma}$. Algebraic rearrangement of Eq. (10) and (11) gives, if ω is replaced by $C\dot{\gamma}$,[19]

$$N_1(\dot{\gamma}) = \frac{2}{C^2}G'(C\dot{\gamma}) \tag{12}$$

This relation implies that $N_1(\dot{\gamma})$ and $2G'(\omega)$ have the same shape in a log–log plot. This is not seen in Figure 6. Despite this lack of correlation, the order of magnitude of Eq. (12) follows closely, particularly in the range $1\ s^{-1} < \dot{\gamma} < 100\ s^{-1}$ using $C = 0.3$ (Figure 6, where $N_1(\dot{\gamma})$ and $2G'/C^2(C\dot{\gamma})$ are plotted for $T = 105°C$). It must be noted that the constant C was independently measured from η and η' curves. The departure from Eq. (12) is noticed at high shear rates. The difference in shape between these two curves may be due to inertial effects. Contrary to the measurement of normal forces, where an analysis of the effect of inertia was performed, there is no such clear analysis in the case of ERD measurements. The only work reported thus far on this subject concerns only Newtonian fluids.[21]

This study was initiated as a contribution to understand the limited Young's modulus E obtained upon spinning cellulose. It seems that despite a theoretical Young's modulus of 250 GPa for cellulose, all the experiments performed so far give $E = 40$ GPa.[14,22] We have become interested in the measurement of viscoelastic relaxation times in order to evaluate the reasons for having rather low modulus fibers.

Several relaxation times θ were measured. Some are deduced from the relaxation of the viscometric functions like the viscosity η, the first normal stress difference N_1 for the cone and plate geometry, and F_X and F_Y for the

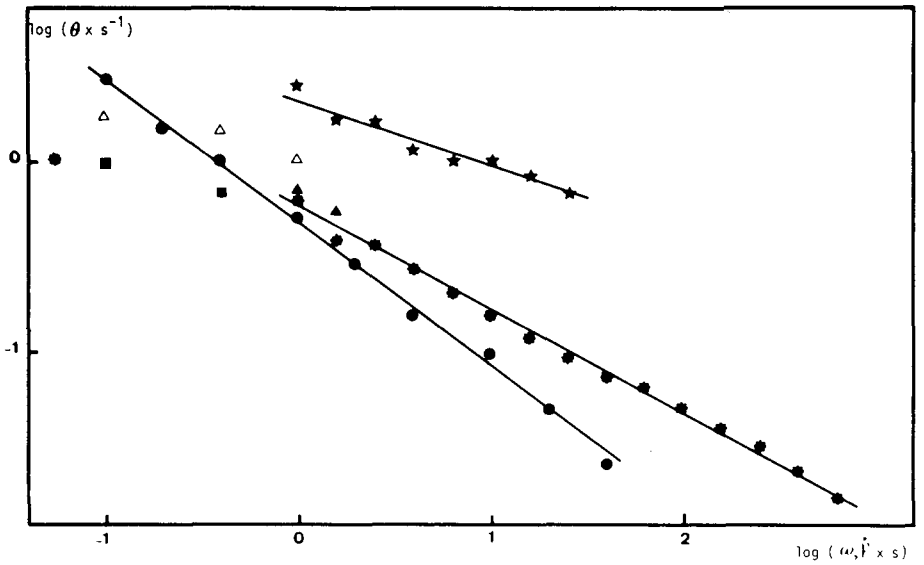

Fig. 7. Relaxation times θ versus frequency ω or shear rate $\dot{\gamma}$ for a 2.5% DMEAO solution at 85°C. △ θF_X; ■ θF_Y; ● θ_M; • θ_N; ★ θN_1; ▲ $\theta\eta$.

ERD geometry. The related relaxation times are, respectively, θ_η, θ_{N_1}, θ_{FX}, and θ_{FY}. Others are part of the constitutive equations. Using a convected Maxwell model gives the relaxation time θ_N and θ_M:

$$\theta_N = N_1/2\eta\dot{\gamma}^2 \tag{13}$$

$$\theta_M = \eta''/G'' = G'/\omega^2\eta' \tag{14}$$

A comparison of these different relaxation times is made in Figure 7. At low γ or ω, all the θ_i give the same order of magnitude, while the differences widen when $\dot{\gamma}$ or ω increases. In Figure 7, θ_M shows a power law behavior, while G' does not. The 2.5% DMEAO solution at 85°C is a special case since η' does not have a power law behavior, but the ratio of G' and η' shows a power law dependance. An interesting feature is presented in Table I where the value of the slope of log θ_N versus log $\dot{\gamma}$ is presented. Despite the fact that the power law index of η versus $\dot{\gamma}$ and N_1 versus $\dot{\gamma}$ are strongly dependent on the temperature and the concentration (see Fig. 3), the slope of log θ_N versus log $\dot{\gamma}$ is a constant. This means that the factors governing the dependance of N_1 and η are the same. This is predicted by the Spriggs' model,[18,19] but with a

TABLE I
Slope of log θ_N Versus log $\dot{\gamma}$ for DMEAO Solutions

Concentration	75°C	85°C	95°C	105°C
1%	−0.68	−0.67	−0.73	−0.68
1.6%	−0.70	−0.70	−0.69	−0.71
2.5%	−0.66	−0.60	−0.69	−0.69

correlation between N_1 and η which gives a slope of $\log \theta_N$ versus $\log \dot{\gamma}$ of -2, instead of -0.7 (Table I). This trend is nevertheless qualitatively interesting.

For high modulus fibers, there are two steps, one being the complete orientation of the molecules prior to crystallization and the second the crystallization itself. Only the first step is considered here. One can have two approaches for the calculation of the full extension of the molecules, a spatial approach and a time one. The spatial approach relates the draw ratio to the dimension of the molecule.[23,24] This analysis is performed for a simple molecule and not for dilute solution and its application is difficult. The time approach is related to relaxation times. With all the restrictions developed above, it has been postulated that a tendency for full extension is obtained when

$$\dot{\alpha} > \frac{1}{b\theta} \tag{15}$$

θ is the relaxation time, b is a parameter being between 1 and 4 depending on the model used[25-27] and $\dot{\alpha}$ is the stretch rate. We will now use a speculative approach to apply Eq. (15). Since we do not have the values of the rheological relaxation time of an elongational deformation, we will use the ones determined in shear. The parameters of the spinning line give the maximum stretch rate of the filament, 200 s^{-1}. Using this short cut we took θ as being the shear relaxation time for $\dot{\gamma} = \dot{\alpha} = 200\ s^{-1}$, which gives $\theta = 0.04$ s (Fig 7). Taking $b = 1$ shows that Eq. (15) is satisfied. According to it, the spinning of these solutions should give a good extension of the chains. Of course, the problem is much more complicated and the influence of the solvent is probably the most important parameter. Disorder will occur upon the exchange solvent-nonsolvent in the coagulating bath.

CONCLUSION

Not many rheological investigations of cellulose solutions can be found in the scientific literature. This is due mainly to the lack of suitable solvents and the fundamental knowledge of the dynamics of the most common natural polymer is very poor. The present study was performed to gain some information on the viscoelastic behavior of high molecular weight cellulose since several organic solvents are now available. One of the two most noticeable results of this study is the astonishing ability of the cellulose—MMNO or DMEAO solutions to stay in the cone-and-plate gap up to very high rotational speeds. The reason is unclear to the authors, but since it is a general behavior for cellulose–organic solvent solutions, and no artifact can be found, a more careful study of this phenomenon is planned. The second result is the qualitative correlation between the results and the Spriggs' theory. Since we were unable to measure the Newtonian viscosity, a qualitative comparison with phenomenological theories is difficult. One way to overcome this problem would be to find a way to get good monodisperse fractions. But since the problem of measuring molecular weights of cellulose is not completely solved, to be able to have fractions is improbable in the near future. This will hamper progress in cellulose rheology.

We are indebted to Dr. M. Little for his help in the preparation of the manuscript and to Dr. J. F. Agassant for useful comments and discussions on this work.

References

1. D. Henley, *Arkiv Kemi*, **18**, 327 (1962).
2. E. Riande and J. M. Perena, *Makrom. Chem.*, **175**, 2939 (1974).
3. H. Chanzy, M., Dube, and R. H. Marchessault, *J. Polym. Sci., Polym. Lett. Ed.*, **17**, 219 (1978).
4. H. Chanzy, A. Peguy, S. Chaunis, and P. Monzie, *J. Polym. Sci., Polym. Phys. Ed.*, **18**, 1137 (1980).
5. H. Chanzy, S. Nawrot, A. Peguy, P. Smith, and J. Chevalier, *J. Polym. Sci., Polym. Phys. Ed.*, **20**, 1909 (1982).
6. H. Chanzy, P. Noe, M. Paillet, and P. Smith, *J. Appl. Polym. Sci., Appl. Polym. Symp.*, **37**, 239 (1983).
7. P. Navard and J. M. Haudin, *J. Therm. Anal.*, **22**, 107 (1981).
8. E. Maia, A. Peguy, and S. Perez, *Acta Cryst.* **B37**, 1858 (1981).
9. E. Maia, A. Peguy, and S. Perez. *Can. J. Chem.*, **62**, 6 (1984).
10. C. C. McCorsley and J. K. Varga, Belg. Pat. 819,735 and 868,736 (1978).
11. P. Navard and J. M. Haudin, *Polym. Process Eng.*, **3**, 291 (1985).
12. P. Navard and J. M. Haudin, *Br. Polym. J.*, **12**, 174 (1980).
13. P. Navard and J. M. Haudin, in *Cellulose: Structure, Modification and Hydrolysis*, R. A. Young and R. M. Rowell, eds., J. Wiley, New York, 1986, p. 247.
14. H. Chanzy, S. Nawrot, S. Perez, and P. Smith, Proceedings of the TAPPI International Dissolving and Speciality Pulps Conference, Boston, 127–132 (1983).
15. P. Avenas, J. F. Agassant, and J. P. Sergent, *La Mise en Forme des Matières Plastiques, Technique et Documentation*, Lavoisier, Paris, 1982.
16. W. M. Kulicke, G. Kiss, and R. S. Porter, *Rheol. Acta*, **16**, 568 (1977).
17. W. W. Graessely, *Adv. Polym. Sci.*, **16**, 1 (1974).
18. T. W. Spriggs, *Chem. Eng. Sci.*, **20**, 931 (1965).
19. S. Middleman, *The Flow of High Polymers*, Interscience, New York, 1968.
20. C. D. Han, *Rheology in Polymer Processing*, Academic Press, New York, 1976, Chap. 5.
21. T. N. G. Abbot and K. Walters, *J. Fluid Mech.*, **40** (1), 205 (1970).
22. I. Quenin, H. Chanzy, M. Paillet, and A. Peguy, *Proceedings of the International Discussion Meeting. Integration of Fundamental Polymer Science and Technology*, Limburg (Netherland) 14–18 April 1985, Elsevier, London (in press).
23. T. Kanamoto and R. S. Porter, *J. Polym. Sci., Polym. Lett. Ed.*, **21**, 1005 (1983).
24. P. Smith, R. R. Matheson, and P. A. Irvine, *Polymer*, **25**, 294 (1984).
25. S. Daoudi, *J. de Physique (Paris)*, **36**, 285 (1975).
26. J. M. Dealy, *Polym. Eng. Sci.*, **11**, 433 (1971).
27. G. Marrucci, *Polym. Eng. Sci.*, **15**, 229 (1975).

Received February 13, 1986
Accepted February 18, 1986